Assembly, Loading, and Cool-down of the FRESCA2 Support Structure

J. E. Muñoz Garcia, C. Giloux, D. T. Ziemianski, F. Rondeaux, G. de Rijk, H. Bajas, J. M. Rifflet, J. C. Perez, M. Durante, M. Charrondiere, M. Bajko, M. Devaux, M. Guinchard, P. Ferracin, P. Fessia, P. Manil

***Abstract* — This paper reports on the assembly process and cool-down to cryogenic temperature of the support structure of FRESCA2, which is a dipole magnet for upgrading the actual CERN cable test facility FRESCA.**

The structure of the FRESCA2 magnet is designed to provide the adequate pre-stress, through the use of keys, bladders, and an Al alloy shrinking cylinder. In order to qualify the assembly and loading procedures, the structure was assembled with Al blocks (dummy coils) that replaced the brittle Nb_3Sn coils, and then cooled-down to 77 K with liquid nitrogen. The evolution of the mechanical behaviour was monitored via strain gauges located on different components of the structure (shell, rods, yokes and dummy coils).

We focus on the expected stresses within the structure after assembly, loading and cool-down. The expected stresses were determined from the 3D finite element model of the structure. A comparison of the 3D model stress predictions with the strain gauge data measurements is made. The coherence between the predicted stresses with the experimental gauge measurements will validate the FEM model of the structure.

***Index Terms*—dipole, EuCARD, magnet, Nb_3Sn, superconducting accelerator magnet.**

I. Introduction

The European Coordination for Accelerator Research and Development (EuCARD [1]) aims at new concepts and technologies for upgrading European accelerators: the High Field Magnet task [2] focuses on designing, building and testing a dipole magnet with operational flux density of 13 T in a 100 mm bore. This 1.5 m long dipole called FRESCA2 will be used to upgrade the FRESCA test facility at CERN, fulfilling the need to qualify conductor at higher fields. Following the description in detail about the design of this magnet in [3], the present paper summarizes the status of the mechanical characterization of the FRESCA2 support structure; describing the first assembly and pre-loading with Al dummy coils. Strain gauge data measurements were obtained at all stages then compared with expected stress values issued from Ansys® calculations. The whole assembled structure was cooled down to cryogenic temperature. We report on the comparison of the experimental strain gauge measurements with the expected FEM strain values. An overview of the magnet development status is given in [4].

Manuscript received on July 17TH, 2013. The research leading to these results has received funding from the European Commission under the FP7 Research Infrastructures project EuCARD, grant agreement no. 227579.

J. E. Muñoz Garcia, C. Giloux, D. T. Ziemianski, G. de Rijk, H. Bajas, J. C. Perez, M. Charrondiere, M. Bajko, M. Guinchard, P. Ferracin and P. Fessia are with CERN CH-1211 Geneva 23, Switzerland (corresponding author phone +41 2276 62001; e-mail jorge.enrique.munoz.garcia@cern.ch).

F. Rondeaux, J. M. Rifflet, M. Durante, M. Devaux and P. Manil are with CEA Saclay, 91191 Gif-sur-Yvette, France

II. Mechanical Design

A. Cross-section

The cross-section of FRESCA2 is shown in Fig. 1. The 100 mm aperture is given by the assembly of two inner central posts, without any additional component. Titanium alloy has been chosen in the central region because of its high strength, also in tension, and for its thermal contraction behaviour; the iron post comes from magnetic considerations.

The coil is surrounded by pads in the horizontal and vertical directions. These pads transfer forces to the outside split iron yoke through keys mostly in the perpendicular directions. These forces on the iron are contained by a 65 mm thick Al alloy cylinder (shell). Two lateral keys per side are used: in this way, the forces are better aligned with the coil, especially around the ends.

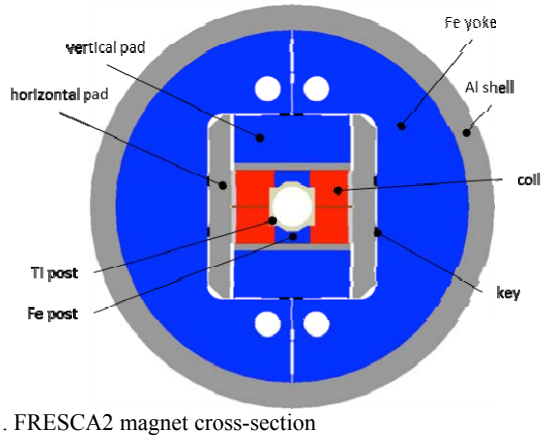

Fig. 1. FRESCA2 magnet cross-section

The mechanical structure was based on the bladder and key concept, approach developed at LBNL [5] and successfully used in several model magnets.

Pre-stress of the coil is provided during cool-down through most of the shrinkage of the shell, and the Lorentz forces will tend to separate the coils during powering. The mechanical design aims at providing adequate pre-stress to the coil, in particular limiting peak stresses at cryogenic temperatures and maintaining the cable under compression along the central posts at the nominal current, providing loading also at full Lorentz forces. The horizontal pad is made of stainless steel; the vertical pad is made of two parts: a stainless steel plate in contact with the coil and an iron insert along the straight section. Ferromagnetic components are shown in Fig**. 1**: the central post, part of the vertical pad and the yoke. The main effect of the iron in the vertical pad and in the yoke is to increase the field in the aperture for a given current. The mass

of the magnet is around 10 t; the yoke contributes with more than 5 t and the shell less than 1 t.

B. Dummy Coils

The coil design of this magnet is based on a block layout [6]; each pole is made of four layers, wound as two double pancakes. For this first assembly and cool-down test, the coil pack was assembled with Al blocks (dummy coils) replacing the brittle Nb_3Sn coils for mechanical testing purposes of the support structure only; they are not intend to represent the behaviour of superconducting Nb_3Sn coils. Fig. 2 shows the two dummy coils one over the other, and the corresponding vertical pads. Both vertical and horizontal pads were bolted around the dummy coils and stacked together.

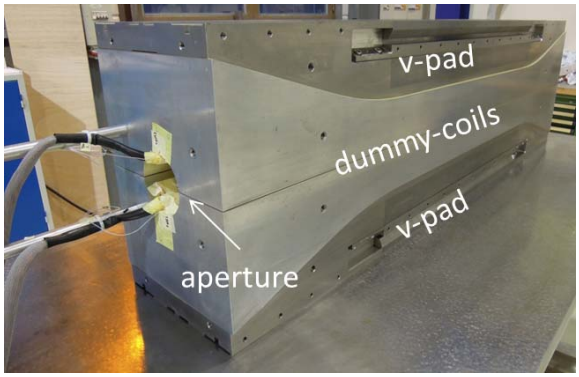

Fig. 2. Dummy coils and vertical pads

C. Longitudinal Compression System

A longitudinal pre-compression system similar to the one of HD2 [7] and SMC [8], was used: four Al alloy rods are pre-tensioned and transfer their load to the coil pack by a high resistance steel end plate. This last component is heavily loaded in bending; moreover, its design has to take into consideration the space needed for keys, bladders, as well as instrumentation wires out of the coil.

III. Instrumentation

The structure was instrumented with half-bridge strain gauges placed in 10 stations distributed in the straight section and end regions (at 0° and 45° from the mid-plane) on the outer diameter of the shell measuring both along azimuthal and axial direction. Similar distribution of 7 stations was used in the inner radius aperture of the dummy coils. All gauges were thermally compensated by gauges mounted on stress-free Al elements. For the dummies these compensators were mounted not in the aperture, but at the exterior. The rods were instrumented with full-bridge strain gauges mounted in opposite azimuthal locations in order to compensate bending effects and they were thermally auto-compensated measuring in the axial direction only. The structure was instrumented with 56 strain gauges in total.

IV. Assembly and Loading

Both assembly and loading procedures were performed similar to other magnets ([9], [10]) as follows: the two yoke-halves were slid into the shell vertically. After inserting two bladders in the slots between the yokes halves, the bladders were pumped in order to spread apart and put in contact the yoke-halves to the internal surface of the shell. The yoke-halves were then aligned and locked with removable inter-yoke keys inserted in the gap between the yoke-halves. At this point the sub-assembly is ready for the following operation: the insertion of the coil pack in horizontal position. After placing the yoke-shell sub-assembly in front of a table, the coil pack was slid in. According to simulations, the nominal horizontal interference for a proper lateral coil preload at 13 T is 0.60 mm obtained with a reasonable pressure in the bladders (in the order of 275 bar). Bladders are inserted next to the key-slots and pressurized, generating a clearance in order to shim the interference keys in the slots before the bladders are removed. As a result the final assembly at room temperature involves interferences.

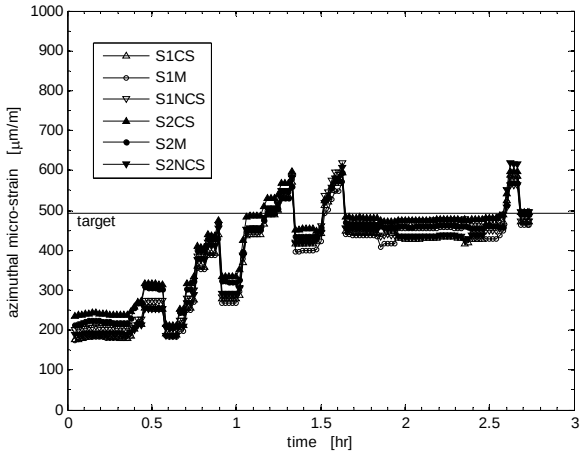

Fig. 3. Assembly test: azimuthal strain on the shell. Half bridge gauges were mounted on two sides of the shell; for side 1 at the middle of the structure (S1M), at connections side (S1CS) and at non-connections side (S1NCS), and (S2M), (S2CS) and (S2NCS) respectively for side2.

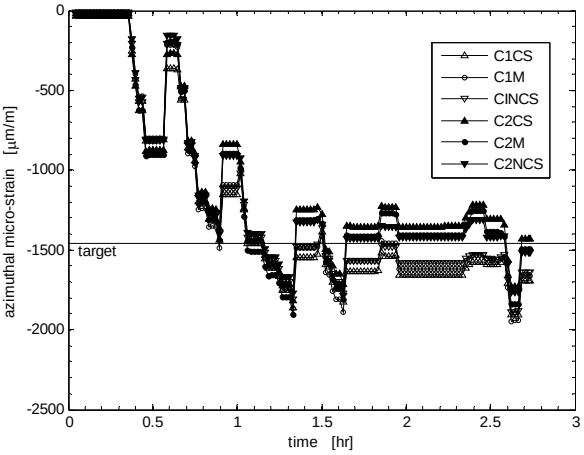

Fig. 4. Assembly test: azimuthal strain on the dummy coils. Half bridge gauges were mounted on the two dummies; for dummy 1 at the middle of the structure (C1M), at connections side (C1CS) and at non-connections side (C1NCS) of the straight section, and (C2M), (C2CS) and (C2NCS) respectively for dummy 2.

These interference values, the size of the keys to tight the structure, were adjusted during bladder operation of the assembly to tune the pre-stress of the coil pack as we can see in Fig. 3 and Fig. 4 for the shell and for the dummy coils respectively: bladders were pumped to be able to insert the shims in the slots; the pressure was then released to verify the strain values, then bladders were pumped again to increase the shimming many times up to the target value.

After bladder deflation, the keys lock the generated clearance, thus ensuring tight contact between components. Fig. 3 and Fig. 4 show that the azimuthal strain measurements reached the chosen target values at room temperature. Both 2D and 3D ANSYS® finite element modelling were performed to analyse the mechanical behaviour of the structure, focusing in particular in locations where strain gauges were mounted. An overall friction coefficient of 0.2 was assumed. So, a target shell azimuthal strain value of 495 μm/m, which corresponds to 35 MPa, was expected and an average of 485 μm/m was obtained. The expected strain value for the dummy coils is 1460 μm/m corresponding to 100 MPa, and an average of 1570 μm/m was obtained for this first assembly.

Finally, the longitudinal compression system is assembled and pre-loaded with a hydraulic tensioning fixture. The structure completely assembled is shown in Fig. 5.

Fig. 5. FRESCA2 structure completely assembled

V. Cool-down

For the cooling down of the FRESCA2 structure at 77 K, a novel nitrogen test facility has been set up in the outside of SM18 building at CERN. The facility is composed of a cryostat (4.57 m high and 1.2 m large formerly used for RF cavity test) placed in a mechanical steel trellis (5 m high and 1.102 m wide) to effectively support the magnet weight. The magnet is hanging below a steel tool yoke that is then set down on the top of the trellis for magnet insertion.

A cryostat insert has been manufactured which includes steel cover, thermal shielding, nitrogen inlet/outlet flanges, safety valves and path for instrumentations. Scaffolding has been mounted around the installation to access to the top of the structure.

To produce nitrogen flow of 25 g/s at controlled temperature (from liquid at 77 K to gas up to 350 K), the Magnet Flushing Station (MFS) has been recuperated from LHC main magnet series tests activity. It contains 5 kW evaporator and 5 kW heaters. Two cryogenics double-wall lines connect the nitrogen main tank to the MFS, and the MFS to the cryostat bottom passing through the magnet aperture. The gas outlet line is wrapped with heaters in order not to ice the outlet.

To empty the cryostat, 5 kW heaters have been placed at the bottom of the magnet. The cooling speed is regulated automatically with respect to the maximum allowable gradient of $\Delta T = 100$ K (to limit the thermal stress from the differential shrinkage of the materials) controlling the evaporator and heaters powers and the liquid nitrogen (LN_2) inlet valve opening.

The temperature of the structure has been measured by Carbon-ceramic sensors mounted on different components of the structure. The $\Delta T = 100$ K was almost reached at the beginning of the cooling-down only between the top and bottom of the rod instrumented with temperature sensors as shown in Fig. 6 (top: solid line, bottom: dashed line), due to the high thermal coefficient of the Al. For the rest of the components the ΔT was lower than 20 K in average during the whole test. One of the temperature sensors has been placed at the middle of one dummy coil (TDM1), location which is the centre of the whole structure; where the mid-temperature was obtained as shown on the same figure.

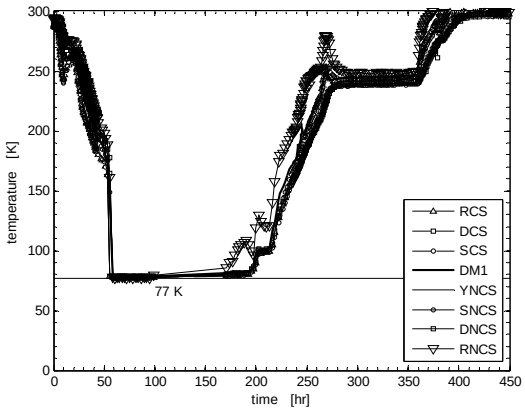

Fig. 6. Temperature during the cool-down test: sensors were mounted on one of the rods at connection side (RCS) and non-connections side (RNCS), dummy coil 1 (DM1), yoke (YNCS) and shell at connections side (SCS) and at non-connections side (SNCS)

The cooling-down has lasted 48 hr injecting gas at T~130 K then LN_2 when the top of the magnet reached 180 K (filling the cryostat in 5 hr maintaining the magnet at 77 K).

Notice that the thermal cycle time has been optimized with respect to the convective heat exchange reducing the interstice between the cryostat inner wall and the magnet from 36 mm to 10 mm to reduce the cross-sectional area for the gas flow. The gas temperature is probed at the MFS outlet, at the middle and bottom of the cryostat.

The warming up has lasted 6 days as shown in Fig. 6, by using gas at 300 K and full power of the cryostat heater. At some point the temperature at the bottom of the rod (RNCS) increased because this location was very close to the heater. Therefore, the heater was turned off in order to stabilize the temperature of the whole structure; this is the reason a plateau is observed. After that the structure was warmed up to room temperature. For the complete cycle, the limit of $\Delta T = 100$ K

was never reached. The temperature signals were in good agreement with expectations.

VI. Analysis

Yoke, dummy coils and support shell stresses are all within acceptable limits during all stages of assembly. The evolution of the shell strain is shown in Fig. 7. The data measurements average at 77 K is 1255 ± 85 μm/m and the corresponding target value is 1460 μm/m (100 MPa). After the warm-up, there is a difference of the strain measurements average of 370 ± 115 μm/m at 293 K in comparison of target of 495 μm/m (35 MPa). The strain after the warm-up is 130 μm/m lower than the measured before the cool-down test. A possible cause of this discrepancy currently under investigation could be related to different friction factor between the components with respect to the 0.2 assumed overall in the FEM model.

The dummy coils reached a strain average value of -3510 μm/m and the corresponding target value is -2865 μm/m at 77 K as shown in Fig. 8. An explanation of this could be that there is a bigger compression transmitted from the horizontal pads of the coil pack to the aperture than expected, resulting in a bending effect and increasing the strain at the aperture radius of the dummy coils. An important experimental dispersion was found at cryogenic temperature only. Nevertheless, the values went back to an average of -1530 ± 88 μm/m which is similar to the corresponding target values of -1460 μm/m at room temperature. The strain obtained after the warm-up is 100 μm/m lower than the strain before the cool-down test.

In Fig. 9 is shown the behaviour of the rods. Longitudinal strain gauge data measurement average of 1160 ± 40 μm/m was obtained at 77 K and the corresponding target value is 1300 μm/m. An increase of experimental dispersion among the four rods was observed at cryogenic temperature only. The data measurement average went back to 625 ± 60 μm/m in comparison with the expected value of 750 μm/m (50 MPa) after the warming-up.

The strain after the warm-up is respectively 130 μm/m for the shell, 125 μm/m for the rods and 100 μm/m for the dummy coils, lower than before the cool-down test. A cause could be that the structure did not reach back the original conditions because of the friction of the structure.

VII. Conclusions

A mechanical structure for 100 mm aperture dipole magnet designed as a test station to superconducting cables is proposed. The FRESCA2 structure has been successfully assembled, pre-loaded and cooled-down to 77 K. All the stages of the assembly process have been verified. The support structure has demonstrated to properly support the loading during the assembly process and at cryogenic conditions. A new cryogenic test facility was made for this test. The measured strain values are generally consistent with the FEM model prediction. The discrepancies observed, in particular after the cool-down, are currently under investigation and they will be further verified with a second cool-down test at 77 K.

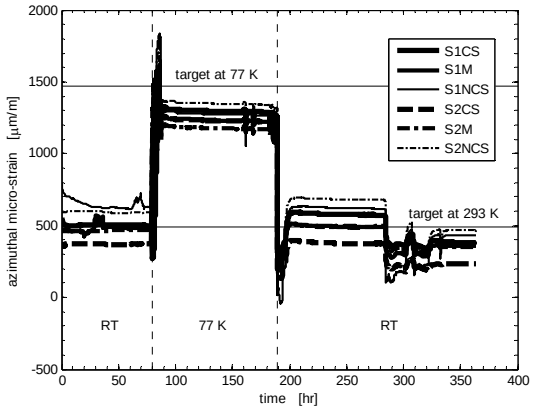

Fig. 7. Cool-down test: azimuthal strain on the shell

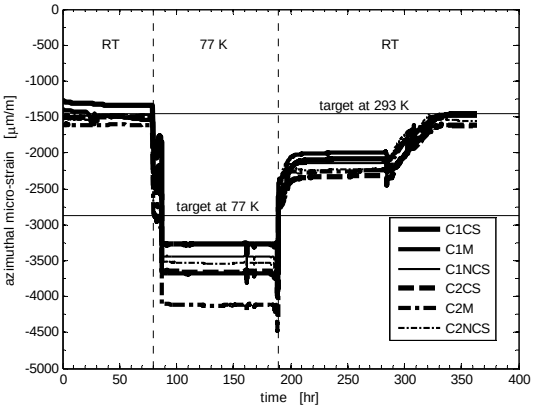

Fig. 8. Cool-down test: azimuthal strain on the dummy coils

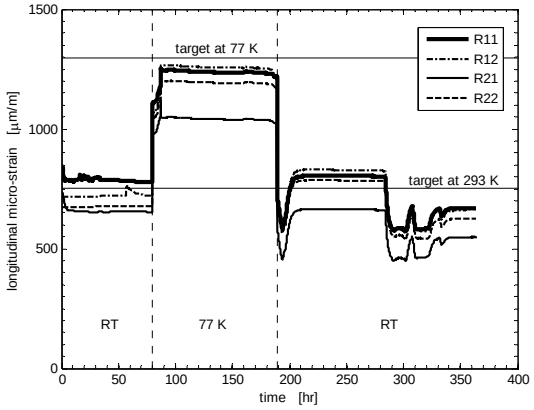

Fig. 9. Cool-down test: axial strain on the rods. Full bridge gauges were mounted on the four rods of the longitudinal compression system

Acknowledgement

We thank all the colleagues with whom we discussed the design of FRESCA2, in particular L. Bottura, L. Rossi, S. Caspi and G. Ambrosio. And for their essential contribution of the cooling system and test station development and operation: P. Viret, V. Benda, D. Willeman and G. Bourgeois.

REFERENCES

[1] G. de Rijk, "The EuCARD high field magnet project" *IEEE Trans. Appl. Supercond*., vol 22, no 3, June 2012.

[2] http://www.ieee.org/publications_standards/publications/authors/authors G. de Rijk, "The EuCARD High Field Magnet project" The EuCARD Project. [Online]. Available: http://eucard.web.cern.ch

[3] P. Ferracin *et al.*, "Development of the EuCARD Nb_3Sn dipole magnet FRESCA2" *IEEE Trans. Appl. Supercond*., vol 23, no 3, June 2013.

[4] P. Manil *et al.*, "Development and fabrication test of the Nb_3Sn dipole magnet FRESCA2" submitted for publication in *IEEE Trans. Appl. Supercond*., vol 24. June 2014.

[5] S. Caspi *et al.*, "The use of pressurized bladders for stress control of superconducting magnets," *IEEE Trans. Appl. Supercond.*, vol. 11, no. 1, pp. 2272-2275, 2001.

[6] A. Milanese *et al*., "Design of the EuCARD high field model dipole magnet FRESCA2" *IEEE Trans. Appl. Supercond.*, vol. 22, no. 3, June 2012.

[7] P. Ferracin *et al.*, "Recent test results of the high field Nb_3Sn dipole magnet HD2," *IEEE Trans. Appl. Supercond.*, vol. 20, no. 3, pp. 292-295, June 2010.

[8] J. C. Perez *et al.*, "The SMC (Short Model Coil) dipole: an R&D program for Nb_3Sn accelerator magnets *IEEE Trans. Appl. Supercond.*, vol. 22, no. 3, June 2012.

[9] P. Ferracin *et al.*, "Assembly and test of a support structure for 3.6m long Nb_3Sn trace track coils" *IEEE Trans. Appl. Supercond*., vol 18, no 2, pp.167-170, June 2008.

[10] P. Ferracin *et al.*, "Assembly and loading of LQS01, a Shell-based 3.7m long Nb_3Sn quadrupole magnet for LARP" *IEEE Trans. Appl. Supercond*., vol 18, no 2, pp.279-282, June 2010.

[11] V. Datskov *et al.*, "Precise thermometry for next generation LHC superconducting magnets" submitted for publication in *IEEE Trans. Appl. Supercond.*, vol 24. June 2014.